

NATIONAL AERONAUTICS AND SPACE ADMINISTRATION  
CONTRACT NO. NAS 7-918

TECHNICAL SUPPORT PACKAGE

on

COMBUSTION OF DROPS OF  
LIQUID FUEL IN A VORTEX

for SEPTEMBER 1994

NASA TECH BRIEF Vol. 18, No. 9, Item #17

from

JPL NEW TECHNOLOGY REPORT NPO-18973

**Inventor(s):** F. G. Fichot  
K. G. Harstad  
J. Bellan

**New Technology Report**  
**Prepared by:** C. J. Morrissey

**TSP assembled by:**  
**JPL Technology Utilization Office**

pp. i, 1-15

NOTICE

Neither the United States Government, nor NASA, nor any person acting on behalf of NASA:

a. Makes any warranty or representation, express or implied, with respect of the accuracy, completeness, or usefulness of the information contained in this document, or that the use of any information, apparatus, method, or process disclosed in this document may not infringe privately owned rights; or

b. Assumes any liabilities with respect to the use of, or for damages resulting from the use of, any information, apparatus, method or process disclosed in this document.

JET PROPULSION LABORATORY  
CALIFORNIA INSTITUTE OF TECHNOLOGY  
PASADENA, CALIFORNIA

SEPTEMBER 1994

## **Combustion of Drops of Liquid Fuel in a Vortex**

A paper discusses a numerical simulation of unsteady evaporation and combustion of drops of liquid fuel clustered in a vortex. This simulation represents the behavior of drops and the combustion processes that occur in large, coherent vortices in the shear layers of liquid-fuel sprays in air.

*This work was done by Floriah G. Fichot, Kenneth G. Harstad, and Josette Bellan of Caltech for **NASA's Jet Propulsion Laboratory.***

NPO-18973.

## Unsteady Evaporation and Combustion of a Drop Cluster Inside a Vortex

F. FICHOT,\* K. HARSTAD, and J. BELLAN†

*Jet Propulsion Laboratory, California Institute of Technology, Pasadena, CA 91109*

A model has been developed that describes the evaporation, ignition, and combustion of a drop cluster embedded in a large vortex. The purpose of this model is to simulate the behavior of drops in large coherent vortices produced in the shear layer of a jet. The model treats the dynamic interactions between the drops and the vortex, and also takes into account the drop proximity to calculate the heat and mass transfer between drops and ambient gas. The gas phase outside the cluster is treated as an unsteady, reacting phase, whereas quasi-steadiness is assumed between the drops and surrounding gas inside the cluster. It is assumed that drops will not burn individually, but as a group. The results show a very complex interaction between the dynamics of the drop-loaded vortex, the flame, and the evaporation process. A quasi-steady state is not always reached, depending upon the drop number density or the vortex intensity. In most cases, the flame is located very close to the cluster. The mass ratio of burned fuel (at complete evaporation) to initial fuel is generally less than 10%.

### NOMENCLATURE

$\alpha_{ent}$	entrainment constant	$R_0(R_0^0)$	cluster outer radius (initial cluster outer radius)
$A$	preexponential factor	Re	Reynolds number
$A_{xy}$	irrotational velocity coefficient	$R$	average gas constant
$B_{xy}$	rotational velocity coefficients	$\rho$	gas density
	$x = g$ (gas) or $d$ (drop)	$s$	stoichiometric coefficient
	$y = r$ (radial) or $\theta$ (tangential)	$t$	time
$C_p$	specific heat at constant pressure	$\tau_{ev}, \tau_{ta}$	evaporation time, turnaround time
$D$	gas diffusivity	$T$	temperature
$d_0$	initial diameter of the drops	$T_a$	activation temperature
$\epsilon$	turbulent kinetic energy dissipation rate	$T_\infty$	ambient temperature
$K_{ev}$	$D^2$ law constant	$u_0$	longitudinal velocity of the vortex
Le	Lewis number	$u_{xy}$	velocity (same subscripts as $A_{xy}$ and $B_{xy}$ )
$l_k$	Kolmogorov scale	$u'$	mean velocity fluctuation
$L_T$	integral scale	$\dot{w}$	reaction rate
$\lambda_T$	Taylor microscale	$Y_f, Y_o$	fuel and air mass fractions
$N$	drop number by unit of vortex length	$z$	nondimensional space coordinate
$n_0$	ambient drop number density		
$\nu$	gas viscosity		
$\Phi$	air/fuel mass ratio		
$r$	radial position from center of the cluster		

### INTRODUCTION

Many recent experiments on liquid fuel sprays have shown that the behavior of the drops is strongly dependent upon the large scale vortical structures created in the shear layers of the jet. Evidence of such behavior was found in the

\*On partial leave from Laboratoire EM2C; CNRS-Ecole Centrale Paris, France.

†Corresponding author.



experimental observations made by Lazaro and Lasheras [1], in a plane, two-dimensional, turbulent mixing layer formed between a uniform liquid spray and a stagnant air flow. Their results show that the large, coherent vortices determine the drops' distribution in the mixing layer, and control the entrainment of air into the spray. Similar observations were made by Crowe et al. [2], who have shown that the Stokes number quantifies the interaction between the drops and the vortex. For  $St = O(1)$ , the drops stay in the same vortex, but they have a finite slip velocity with respect to the gas. This is the situation modeled in this paper.

Recently, Longmire and Eaton [3] have studied experimentally the precise interactions between particles and a jet dominated by vortexing structures. They have found that vortices govern the local particle concentration and dispersion, and that this mechanism is strong enough to persist at high particle-to-gas mass ratios. All these experiments clearly show that for most practical sprays, drops entrained in large vortices are a characteristic feature that a realistic modeling of spray combustion should take into account.

The purpose of the present model is to describe the ignition, evaporation and combustion of a group of drops inside a vortex. The first question addressed here is that of the location at which ignition will occur. The previous work of Bellan and Harstad [4] showed that a mixture of fuel and oxidizer accumulates in the center of the vortex as the drops centrifuge and form a ring, but that the temperature is too low to initiate reaction. The low temperature was the result of the dense collection of drops acting as an energy sink on the gas, and heat transfer from the cluster surroundings being too slow to compensate for the energy conducted to the drops. Presumably, ignition will take place where the temperature is maximum because of the high sensitivity of the reaction rate to the temperature. In our model, combustion occurs at the periphery of the cluster, where the temperature is high, and fuel and air are already present. This ignition process is different from the ignition of a gaseous diffusion flame described by Linan [5] because in that work air and fuel were already mixed (though in two different phases).

In the present model ignition may start in the gas phase inside the cluster, with the onset of the reaction being at the periphery of the sphere of influence [4], or at the cluster periphery; in the first case the flame moves quickly to the cluster boundary, although this flame motion is here inferred, and it is not described by the model. The sphere of influence is defined around each drop as being centered at the drop center and having a radius equal to the half distance between the centers of two adjacent drops (the cluster is monodisperse). Thus, the entire cluster volume is the ensemble of all spheres of influence plus the space between the spheres of influence. The space between the spheres of influence is called the interstitial space. In a recent paper, Rangel and Continillo [6] assumed that a high temperature in the center of a vortex containing drops would prompt ignition in the vortex core. Their assumption may be valid if hot products actually accumulate in the center, as was shown for gaseous combustion in vortices by Karagozian and Marble [7], or by Ghoniem et al. [8], but may be questionable when drops are present, especially for dense clusters of drops.

Following ignition, we assume that combustion occurs in a cylindrical flame around the cluster consistent with our assumption of axisymmetry in the axial direction of the vortex [4]. The distance between this flame and the cluster is of interest because it is a scale that allows the characterization of the effects of smaller scale turbulence such as the one that builds up inside the large vortex. Other interesting characteristics are the effects of the dynamics of the vortex on the drops, and hence, on the flame, the validity of a quasi-steady assumption in the outer gas phase, and the fraction of initial fuel that has burned before complete evaporation of the drops. All this information is important because it is an inherent part of the modeling of jet spray combustion.

The present paper introduces a model and a numerical method to study the influence of various characteristic parameters of the ambient gas, of the drop cloud, and of the vortex upon the flame. Novel conclusions provide a good understanding of the drop-flame interaction in a vortex.



## MODEL AND NUMERICAL METHOD

The configuration and the mathematical formulation of the vortex and drop cluster dynamics, and the drop evaporation process can be found in Bellan and Harstad [4]. It is a cylindrical cluster of single component fuel (decane), uniformly distributed, monosize drops, embedded into a cylindrical, infinite, vortical structure. Figure 1 is an illustration of the present configuration and the Appendix provides a summary of the assumptions used in this study.

Conservation equations of mass and momentum for both the gas and liquid phase, and conservation equations of fuel and energy for the cluster are used to determine the dynamics of this system and the evaporation process.

The tangential and radial velocities for both the gas and the drops have the form  $u_{xy} = A_{xy}/r + B_{xy}r$ , which is consistent with the continuity and momentum equations [( $x = d$  (drop) or  $g$  (gas), and  $y = r$  (radial) or  $\theta$  (tangential))] except for the drop radial momentum equation which is solved in average [4]. In Bellan and Harstad [4], the ambient gas is

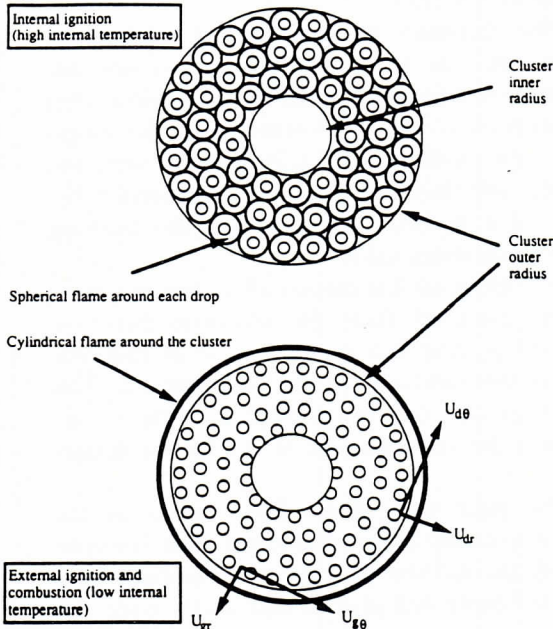


Fig. 1. Schematic view of the cluster at a fixed axial location for internal ignition and external ignition. When internal ignition occurs the flame eventually establishes at the periphery of the cluster.

considered to be uniform in temperature and composition, and the heat and species transfer between the cluster and the outer gas are modeled using the Nusselt number to account for convection and diffusion. The results of that previous study have shown that most of the gaseous fuel will accumulate in the inner part of the cluster, but the temperature will be too low to initiate any reaction. Experimental evidence [9–15] suggests that combustion will occur in the narrow region at the periphery of the cluster where, as it will be shown later, inward convection of fuel (due to cluster expansion) is balanced by outward diffusion.

The purpose of the present study is to model the behavior of the gas phase just next to the cluster surface, in order to determine the existence of a flame, its characteristics, and the resulting effects one can expect when modeling the combustion of jet sprays. In the gas outside the cluster, classic conservation equations are used for the species and the enthalpy, and their solution provides the mass fractions and temperature profiles. Since the cluster surface represents a moving boundary for the equations, we chose to use a new space variable  $z = r/R_0$  (where  $R_0$  is the outer radius of the cluster), for which the cluster surface is always at  $z = 1$ . The conservation equations are as follows:

$$\begin{aligned} \frac{\partial Y_f}{\partial t} + \frac{1}{R_0}(u_{gr} - u_{dr_0}z) \frac{\partial Y_f}{\partial z} \\ = \frac{1}{z\rho R_0^2} \frac{\partial}{\partial z} \left[ \rho z D \frac{\partial Y_f}{\partial z} \right] - \frac{\dot{w}}{\rho}, \end{aligned} \quad (1)$$

$$\begin{aligned} \frac{\partial Y_o}{\partial t} + \frac{1}{R_0}(u_{gr} - u_{dr_0}z) \frac{\partial Y_o}{\partial z} \\ = \frac{1}{z\rho R_0^2} \frac{\partial}{\partial z} \left[ \rho z D \frac{\partial Y_o}{\partial z} \right] - \frac{s\dot{w}}{\rho}, \end{aligned} \quad (2)$$

$$\begin{aligned} \frac{\partial T}{\partial t} + \frac{1}{R_0}(u_{gr} - u_{dr_0}z) \frac{\partial T}{\partial z} \\ = \frac{1}{z\rho R_0^2} \frac{\partial}{\partial z} \left[ \rho z D \frac{\partial T}{\partial z} \right] + \frac{\dot{w}Q}{\rho} C_p. \end{aligned} \quad (3)$$

The two boundary conditions for these equations are values at the outer edge of the cluster



which are obtained from the solution of the cluster conservation equations [4], and ambient values. The values of the gas-dependent variables at the outer edge of the cluster are the same as the interstitial values (assumed uniform; see Appendix) and the same as the values at the edge of the sphere of influence. This is consistent with the concept of this model whereby each drop receives information from the surroundings through the intermediary of its sphere of influence.

The equations are discretized on a uniform mesh, using centered schemes for the space derivatives. A semiimplicit scheme is used for the time derivative. The continuity equation is used together with the equation of state and a constant pressure assumption to calculate the velocity field.

$$\frac{\partial \rho}{\partial t} - \frac{u_{dr_0} z}{R_0} \frac{\partial \rho}{\partial z} + \frac{1}{zR_0} \frac{\partial}{\partial z} [\rho u_{gr}] = 0, \quad (4)$$

$$p = \rho RT. \quad (5)$$

The chemical source terms are calculated with constants for the combustion of decane, found in Westbrook and Dryer [16],

$$\dot{w} = A \rho^{1.75} Y_f^{0.25} Y_o^{1.5} \exp\left(-\frac{T_a}{T}\right), \quad (6)$$

and this term is linearized in the semiimplicit scheme. The time-step is carefully recalculated after each iteration to avoid numerical instabilities.

Knowing the evolution of the profiles during a time step, one calculates the fluxes of fuel, air, and enthalpy from the outer gas phase to the cluster. These fluxes are used then as boundary conditions in the cluster model to calculate the dynamics and the evaporation inside the cluster during this same time step. As a result, new values of the air and fuel mass fractions, and temperature at the cluster boundary are computed and they are introduced in the outer gas calculation to start a new iteration. The computation is stopped when the drops are almost evaporated, that is when the residual drop radius is 10%.

One may notice that the mass fractions and temperature at the outer edge of the cluster play a critical role because they are used as

boundary conditions to solve the previous set of partial differential equations, and therefore to calculate the fluxes from the outer gas phase to the cluster of drops. As stated above, these critical parameters are chosen to have the interstitial values of the mass fractions and temperature, that is, the values at the periphery of the spheres of influence. As already discussed, this is consistent with the assumption that the periphery of the sphere of influence represents also the condition at the periphery of the cluster of drops.

The initial conditions for these interstitial values are chosen to be the ambient conditions. In the outer gas phase, the profiles are initially flat, having the ambient values.

The ambient conditions correspond usually to a mixture of air, a non-reactant gas, without fuel, at a given temperature  $T_{ga}$ . For the drops' motion, two initial parameters were varied (numerically  $A_{g\theta} = B_{d\theta}$ ;  $A_{g\theta}$  in  $\text{cm}^2/\text{s}$  and  $B_{d\theta}$  in  $\text{s}^{-1}$ ) and the others were set to zero (numerically  $B_{g\theta} = A_{g\theta} = B_{gr} = A_{dr} = B_{dr} = A_{d\theta} = 0$ ); this means that the drops are assumed to have initially a purely spinning motion, while the gas motion is initially purely irrotational; the viscous core is assumed infinitesimally thin.

The question of smaller-scale turbulence (compared to the vortical scale) is not addressed in this paper. However, it is likely that a range of scales will interact with the drops, whereas another scale will interact with the flame, and thus it is pertinent to ascertain the role of turbulence in modifying the burning and evaporating rates.

It is assumed that among all turbulent scales, large scales will have the dominant effect on the drops, and this is the only scale that was taken into account in the calculations. This scale (noted  $L_T$ ) is considered to be of the same order of magnitude as the cluster diameter.

This large scale is also likely to act on the flame to create a distorted flame front between the drops and the ambient gas. Smaller scales of turbulence will also stretch and wrinkle the flame front on the boundary of each large vortex, and it is interesting to evaluate the ratio of these length scales to the distance between the flame and the drops, in order to

determine whether they act independently on the drops and the flame.

To evaluate these various scales, we consider the baseline case used for the calculations.

The large scale is  $L_T \approx R_0 = 2.10^{-2}$  m.

The initial tangential velocity of the cluster will be identified with the mean velocity fluctuation  $u'$ .

$$u' \approx \frac{A_{go}}{R_0} = 1 \text{ ms}^{-1}.$$

The dissipation rate of the turbulent kinetic energy is

$$\epsilon \approx \frac{u'^3}{L_T} = 50 \text{ m}^2 \text{ s}^{-3}.$$

The Kolmogorov scale may be estimated, when the gas viscosity is set to  $\nu = 10^{-5} \text{ m}^2 \text{ s}^{-1}$ :

$$l_k = \left( \frac{\nu^3}{\epsilon} \right)^{1/4} = 2.10^{-4}, \quad \text{so} \quad \frac{l_k}{L_T} = 1\%.$$

The turbulent Reynolds number is  $\text{Re}_T = u' L_T / \nu = 2000$ . And the Taylor-microscale is

$$\lambda_T = \sqrt{\frac{15 L_T^2}{\text{Re}_T}} = 2.10^{-3}, \quad \text{so}$$

$$\frac{\lambda_T}{L_T} = 10\%.$$

These ratios will be compared later with the ratio of the distance between the flame and the cluster, to the cluster diameter.

## RESULTS

### General Comments

In a typical run, the temperature inside the cluster decreases, because of cooling induced by the evaporation of the drops which act as heat sinks. Thus the gas will convect toward the vortex core. The drops are entrained with the gas but are also affected by the centrifugal

force which propels them to the outer part of the vortex. The competition between centrifugal force and convection by the gas determines the slip velocity between the drops and the gas. The slip velocity is very important in determining the transfer of mass, species, momentum, and heat between the cluster and the ambient. It is important to notice that convection from the cluster to its surroundings occurs if the drops move inward. In contrast, a substantial diffusion flux from the cluster to the outside is obtained when the drops move outward because this reduces the distance between the ambient and the interstitial conditions, and hence sharpens the gradients. Of course, these simple considerations do not replace a complete calculation, but they help understand the transfer between the cluster and its surroundings.

As hot ambient air is initially in contact with the cluster, and some of this air is assumed to be already mixed with the fuel vapor in the gas phase around each drop, combustion starts as a premixed flame around each drop, spreading to the gas surrounding the cluster as fuel diffuses into the surrounding air. Previous studies [17] show that depending upon the denseness of the cluster, ignition might start internally or externally. In some situations, the flame stays very close to the cluster, implying that burning either occurs mainly inside the cluster or that if burning occurs only outside the cluster, then the flame is weak. The first situation is called "internal combustion," and it occurs when the gas in the cluster is at a high enough temperature to allow the flammable mixture around the drops to burn. However, the main interest here is in situations where "group combustion" occurs, that is, when the flame establishes itself out of the cluster, and the peak reaction rate is large compared with the reaction rate around the drops.

The typical flame configuration in a "group combustion" case is the following: a cold mixture of fuel and air exists near the cluster, followed by a weak premixed flame in the region where the temperature becomes high enough for the gas to ignite, which is itself followed further out by a diffusion flame consuming all the fuel. Although this flame does not consume all of the incoming air, because in



this unconventional situation air arrives at the flame both from the ambient and the cluster, we still call this a diffusion flame.

The fuel flux is determined by the balance between diffusion out of the cluster and convection into the cluster. This means that the flame is located at a position where the Reynolds number based upon the slip velocity and the flame-cluster distance is of order one.

Figures 2a–2d show the situation in a typical run. The intense initial premixed flame may be noticed (see the higher peak in the reaction rate), as well as the clear separation between the diffusion flame (see the lower peak in the reaction rate) and the premixed flame. The incomplete depletion of oxidizer is shown, as

well as the contribution of both flames in increasing the temperature.

### Existence of a Quasi-Steady State

The important parameters quantifying the interaction between combustion and evaporation are the air/fuel mass ratio, the drop number density, and the drop diameter. However, a calculation made with a constant drop number density and two different diameters (20 and 30  $\mu\text{m}$ ) proved that a change in the drop diameter did not change the nature of the combustion (internal or external). Thus, the most important parameter appears to be the drop number density which determines the heating or cool-

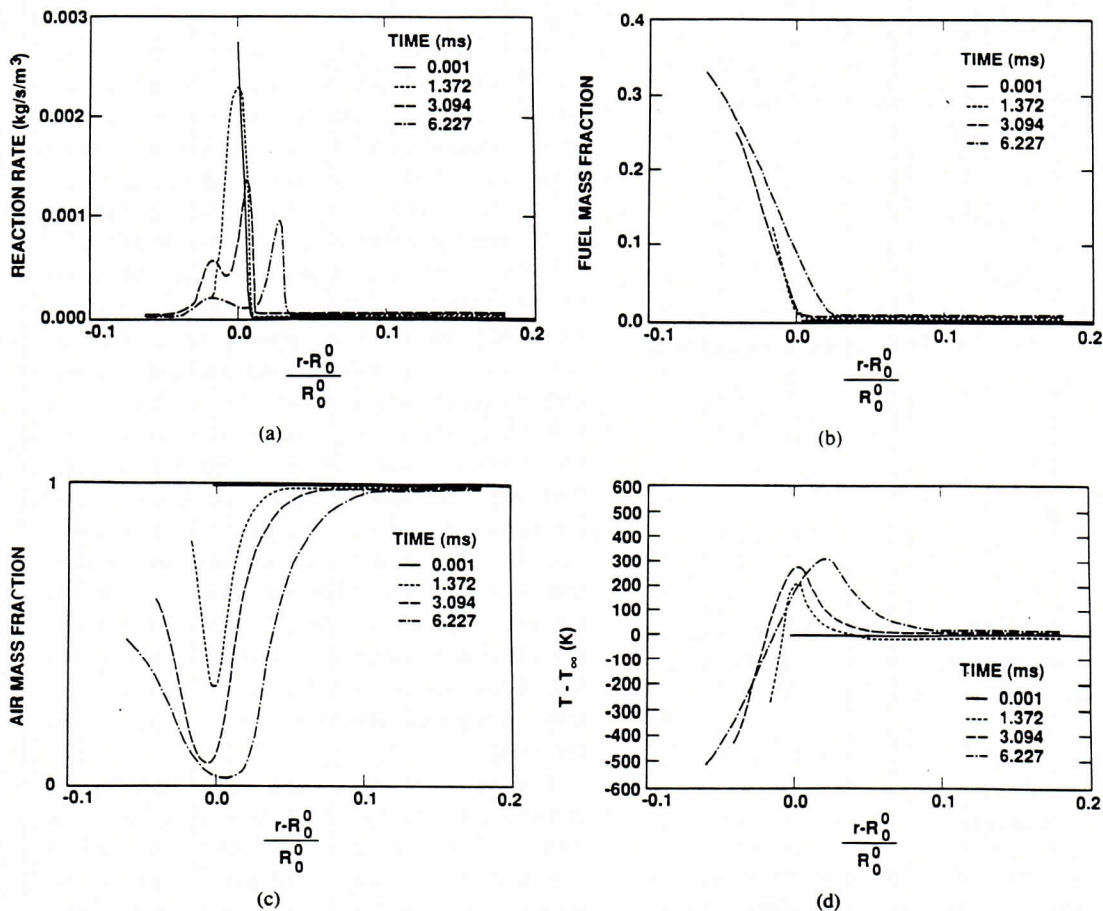


Fig. 2. (a) Variations of the reaction rate as a function of a non-dimensional radial position, for different times. (b) Variations of the fuel mass fraction as a function of a nondimensional radial position, for different times. (c) Variations of the air mass fraction as a function of a non-dimensional radial position, for different times. (d) Variations of the temperature difference with the ambient as a function of a nondimensional radial position, for different times.

ing of the cluster, and therefore the likelihood of internal combustion.

As most of the calculations have shown, a quasi-steady diffusion flame is obtained before complete evaporation of the drops. Thus, the final amount of fuel burned before the drop disappearance (residual radius of 10%) may be estimated by making a comparison between the fuel transport time and the evaporation time. For example, in the 10- $\mu\text{m}$ -diameter case, the evaporation time is so short compared with the diffusion time that only a very small amount of the fuel that has escaped the cluster has been burned, whereas in the 30- $\mu\text{m}$  case, the fuel is burned as fast as it escapes the cluster (Fig. 3).

For the 20- $\mu\text{m}$  drops, changing the ambient temperature does not modify the final behavior of the reaction as evidenced by the curves on Fig. 4 showing the reaction rate reaching an asymptotic limit. This proves indeed that the flame is of the "diffusion type." The final position of the flame is also independent of the ambient temperature, which gives credibility to the idea that a quasi-steady diffusion flame is established before the end of evaporation. The time needed to reach that quasi-steady state is approximately the extinction time of the initial premixed flame. For example, when varying the ambient temperature, with numerically  $A_{g\theta} = B_{d\theta} = 400$ , one can see that the quasi-steady state is hardly reached because the premixed

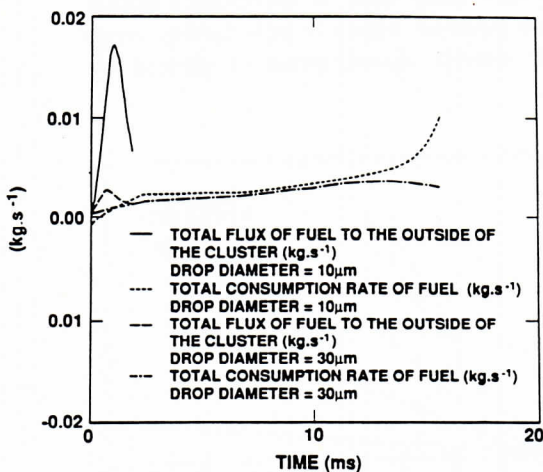


Fig. 3. Comparison between the total flux of fuel escaping the cluster and the total consumption rate of fuel as a function of time, for two drop diameters.

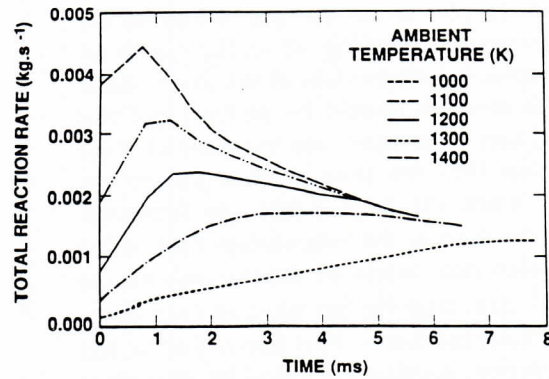


Fig. 4. Integrated reaction rate (over the outer gas volume) as a function of time, for various ambient temperatures ( $A_{g\theta} = B_{d\theta} = 200$ ).

flame is still strong at the end of evaporation (Fig. 5). In most cases, the maximum temperature and the position of this maximum are not constant during the quasi-steady state. The flame is moving away from the cluster, its temperature rising slowly. Both observations may be explained by the depletion of air in the cluster: the flame has to move far from the cluster to find air to continue burning. Being further from the cluster (which acts as a heat sink), the flame increases its maximum temperature. However, in some cases, the position of the flame, or the maximum temperature are rather constant. This is due to the particular conditions and must be considered as a fortuitous result.

#### Parameters Controlling the Quasi-Steady State

In most cases, evaporation is faster than combustion, even for 40- $\mu\text{m}$  drops. This can be

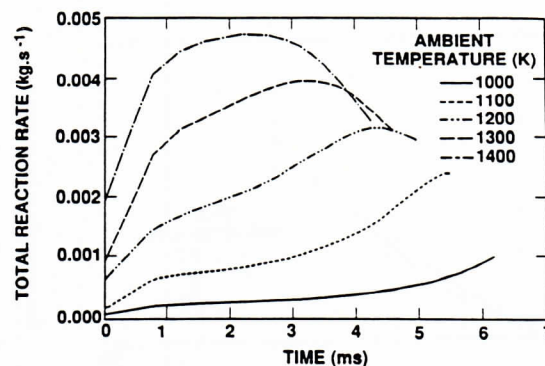


Fig. 5. Integrated reaction rate (over the outer gas volume) as a function of time, for various ambient temperatures ( $A_{g\theta} = B_{d\theta} = 400$ ).



seen on the plot of the fraction of burned fuel as a function of time (Fig. 6): all the curves are superimposed, independent of the drops' diameter. However, it should be pointed out that the air/fuel mass ratio was constant in these cases, and thus the drop number density decreased when the drop radius was increased. Hence the ratio of the evaporation time to the combustion time seems to depend only on the air/fuel mass ratio (in the range of drop diameters considered here). This shows that in this configuration, combustion could be controlled mostly by the diffusion of heat and oxidizer. To verify this conclusion, the diffusivity of the gas was increased. As expected, when the diffusivity is larger, the flame lies further from the cluster and consumes more fuel. Two different calculations were made. In one case the diffusivity was doubled only in the outer gas phase, and in the other case it was doubled both inside and outside the cluster. This would represent for example the effect of small scale turbulence on the transport mechanisms, and the respective situations where turbulence influences only the outer gas, or both the drops and the outer gas. Although doubling the gas diffusivity inside the cluster improves evaporation and causes more fuel vapor to escape to the outside, the fraction of burned fuel is the same in both cases (Fig. 7). This shows that the flame is indeed diffusion-controlled and does not depend on the amount of fuel evaporated in the cluster. This can be explained by the fact that a large amount of evaporated fuel corresponds to a large amount of heat taken by the

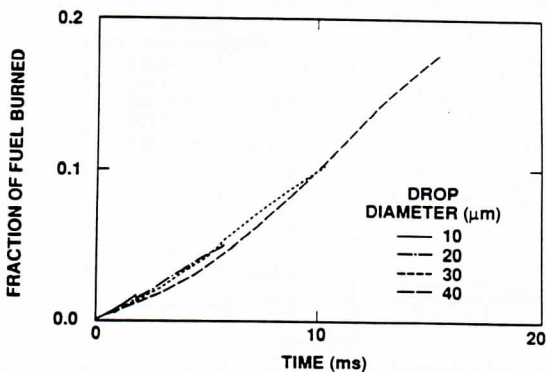


Fig. 6. Fraction of the initial mass of fuel that has burned, as a function of time, for various drop diameters.

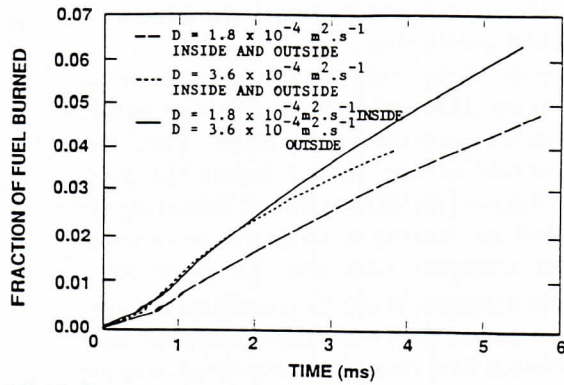


Fig. 7. Fraction of the initial mass of fuel that has burned, as a function of time, for different values of the gas diffusivity inside and outside the cluster.

cluster from the outer gas through the heating and evaporation of the drops, and hence the flame establishes itself further away from the cluster boundary, toward the high temperature air. In this process it is not the flame which is moving, but it is the cluster which is shrinking away from the flame, as the position of flame is more a function of the heat transferred to the cluster than of the amount of mass evaporated. This result was confirmed when the initial air/fuel mass ratio was varied: an almost identical burning rate is observed, leading to a higher final fraction of burned fuel when the air/fuel mass ratio was higher (Fig. 8). However, an increase in the flux of fuel to the region outside of the cluster (as found when the air/fuel mass ratio is decreased) affects the flame position which is now further away from the cluster. Examination of plotted re-

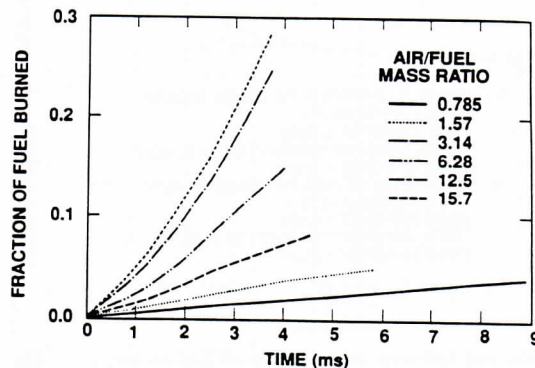


Fig. 8. Fraction of the initial mass of fuel that has burned, as a function of time, for different air fuel mass ratios.



sults reveals that this situation corresponds to a reduced outward velocity of the drops. This reduced outward velocity is evidence of the competition between the movement of the flame toward the ambient (to obtain more high-temperature air) and the movement of the drops going to the flame. This phenomenon will be analyzed more precisely below, when we discuss the effects of the dynamics of the drops upon the flame.

### Internal Combustion Mode

Another interesting point to notice when varying the air/fuel mass ratio is the occurrence of "internal ignition" [17], that is, ignition around each drop in the cluster. Although the present model was not designed to handle internal combustion, some comments may be made, bearing in mind that the results in this case are highly inaccurate, and obviously depend on the size of the mesh. Internal ignition occurs for high air/fuel mass ratios, when evaporation does not cool the cluster sufficiently. Then the inner temperature is high enough to enable a reaction in the interstitial gas phase between the drops. This is represented in the model by a high reaction rate in the first cell of the outer mesh. The combustion is mostly premixed, and consumes a much greater fraction of the initial fuel than in the other cases (up to 30%) (Fig. 8). The quasi-steady diffusion flame is never reached in these situations where the premixed flame dominates, and the flame stays very close to the cluster.

### Effects of the Vortex Dynamics

As it was noticed before, the position of the flame depends greatly on the drops' radial velocity. This is an important parameter which is directly related to the characteristics of the shear layer, through the interactions between the vortex and the drops entrained into it. Hence the initial spinning rate of the drops ( $B_{d\theta}$ ) was varied, as well as the initial vorticity of the gas ( $A_{g\theta}$ ). As expected, the flame is closer to the cluster when the initial drop tangential velocity is higher. However, this motion also brings cold drops to the reaction

zone, cooling the igniting flame. As a result, ignition is delayed. This is easily seen on Fig. 9 showing the maximum flame temperature; each curve reaches the same final temperature with a different delay. When the "cooling effect" of the drops is eventually overcome by the reaction, a substantial amount of fuel has accumulated and mixed near the cluster, and an intense premixed flame starts to burn. There is not enough time left for the quasi-steady diffusion flame to become established, and the final structure of the flame consists of two reaction zones (a premixed flame and a diffusion flame) of similar intensity. Unexpectedly, the fraction of fuel burned increases with the initial spinning rate of the drops. One might have expected that a higher outward velocity of the drops (resulting from a larger centrifugal force) would let less fuel escape to the outside (which is true at the beginning of the calculation), and that the cold drops close to the reaction zone would act as a heat sink. However, the shorter distance between the flame and the drops is also the cause of an increased diffusion flux of fuel to the region outside the cluster. This leads to a higher total flux of fuel at the end of the calculation, and a higher total reaction rate. As we have seen, these effects are alternatively predominant during the combustion process, and there is a critical initial spinning rate for which the initial ignition delay will become too long to enable a significant amount of fuel to be burned in the end. For  $B_{d\theta} = 400 \text{ s}^{-1}$ , the fraction of burned fuel is maximum (Fig. 10).

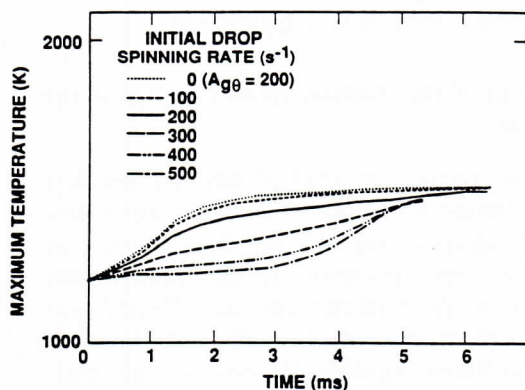


Fig. 9. Maximum temperature in the gas phase as a function of time, for different initial drop spinning rates.

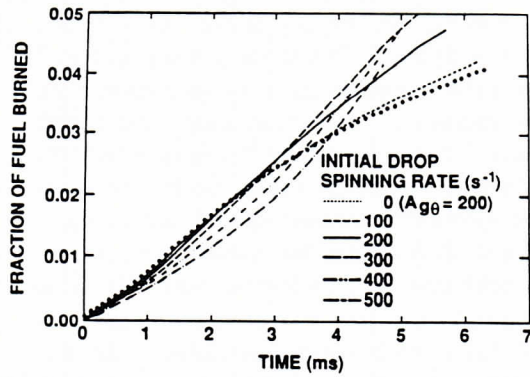


Fig. 10. Fraction of the initial mass of fuel that has burned as a function of time, for different initial drop spinning rates.

**Influence of the Cluster Diameter**

The dynamics of the drops also depends upon the initial radius of the cluster. It turns out that the cluster radius does not have a direct effect on the flame structure, although changing somewhat the drops' dynamics. Except for the 0.5-cm-radius case, the flame is at the same radial distance for a fixed time, and moves outward at the same speed (the distance is here relative to the cluster boundary). The resulting total reaction rate is the same, which may be explained by the identical fuel flux per unit of cluster surface.

Only for the smallest radius studied here (0.5 cm), the cluster is small enough to be quickly heated by the outer gas, rather than cooled by evaporation. Consequently there is no accumulation of cold fuel between the flame and the cluster, and most of the escaped fuel is burned. For this particular case, more than 20% of the initial fuel is burned, whereas less than 10% is burned in a typical run.

**Influence of the Oxidizer Mass Fraction in the Ambient**

The last parameter studied was the oxidizer mass fraction in the ambient. It has been previously noticed that the air flux toward the flame is very important in determining the intensity of the total reaction rate. The calculations confirm this result, as the total reaction rate decreases significantly with the air mass fraction in the ambient. It is also noticed that, as expected, the flame stays further from the

cluster. This influence had already been observed by Koshland [18], but in a different configuration which prevents making accurate comparisons with those observations.

**Drops' Trajectory and Dispersion**

The drops are centrifuged by the vortex, but a strong cooling of the cluster may sometimes prevent an expansion of the cluster. Trajectories of the outer drops have been plotted on Fig. 11 for different initial conditions, and Fig. 12 shows a sketch of the configuration.

As expected, increasing the initial spinning rate of the drops leads to a larger trajectory and a greater radial dispersion. For a lower air/fuel mass ratio, the total evaporation time is larger, and one can see that the drops are first moving inward (following the shrinking of the cluster), and then outward as the centrifugal force eventually overcomes the initial movement. For a larger drop radius (30 μm), but the same drop number density, the total evaporation time is also longer, and the centrifugal force is larger. The resulting trajectory is longer with a large radial dispersion. The effect of the drops' diameter on dispersion was also studied. A definition for the dispersion was chosen to be

$$D_x = \frac{1}{N} \sum_{i=1}^N |x_i - x_{oi}|,$$

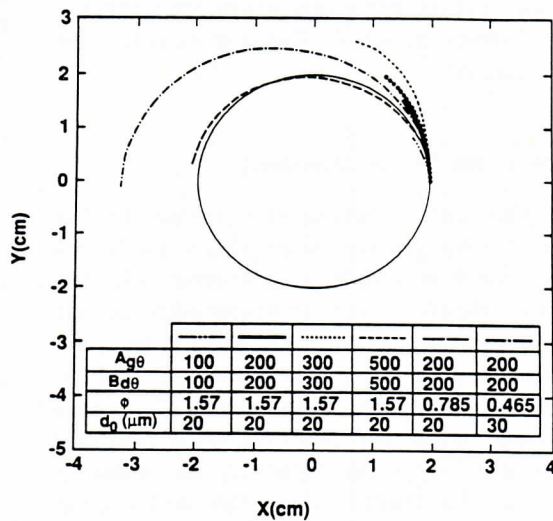


Fig. 11. Trajectory of the outer drops for various conditions.



where  $x_i$  is either the curvilinear abscissa or the radial position of a drop,  $x_{oi}$  being the initial value of the same variable. When  $x$  is the curvilinear abscissa, one can see in Fig. 13a that the dispersion rate increases when the size of the drops decreases. This means that the entrainment of the drops by the gas is more important than the centrifugal force to determine the length of a drop trajectory. This could also be observed on the drop trajectories in Fig. 11. When  $x$  is taken to be the radial position in the above expression, an interesting feature appears: there is a maximum radial dispersion rate for a drop radius between 20 and 30  $\mu\text{m}$ . This can be explained by the fact that small particles follow the gas motion and cannot be centrifuged substantially, whereas large particles can be greatly centrifuged but do not get enough rotational velocity from the gas because of their large inertia. As a result, an optimum exists, for which a maximum radial dispersion rate is obtained (see Fig. 13b).

#### Implications of the Results for Spray Combustion

In a spray or a jet, the entrainment of fluid in the large structure is an important feature. Thus, one should compare results obtained from calculations where no drops are entrained, to the entrainment rate in a spray in order to have an idea about the number of drops and the configuration that one may find in the large structures of a spray.

The time needed to achieve a complete cluster rotation  $\tau_{ia}$ , has to be compared with the evaporation time  $\tau_{ev}$ , in order to find out the approximate trajectory of the drops. If  $\tau_{ev} >$

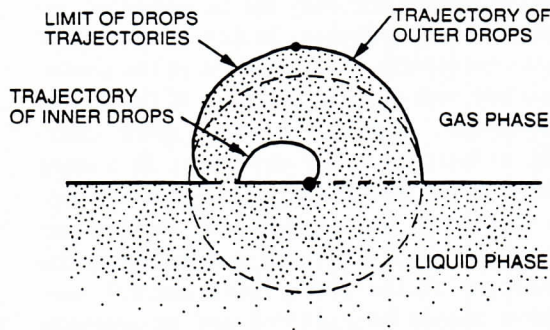
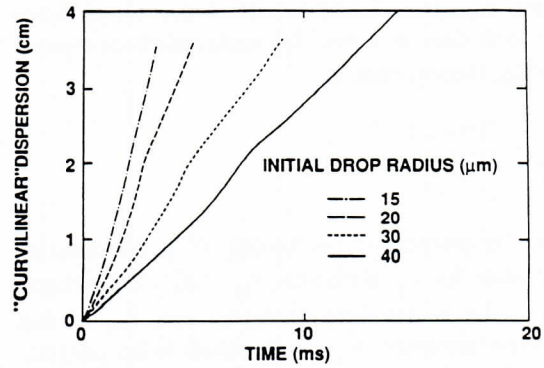
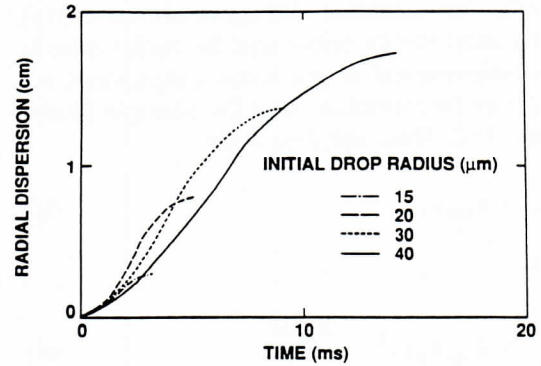


Fig. 12. Sketch of the situation in a large structure of a shear layer.



(a)



(b)

Fig. 13. (a) Average curvilinear abscissa of the drops as a function of time for various drop radii. (b) Average radial displacement of the drops as a function of time for various drop radii.

$\tau_{ia}/2$ , then the drops will be able to get back to the cluster before complete evaporation, and they will form a "ring" in the vortex. If  $\tau_{ev} < \tau_{ia}/2$ , the drops evaporate before being brought back to their initial environment, and they will form tails, as shown in Fig. 12.

The calculations, and the previously shown trajectories indicate that usually  $\tau_{ev} < \tau_{ia}/2$  and one may expect the drops to form tails in agreement with the results found here.

Another characteristic time which is important to compare to the evaporation time is the time governing the entrainment of drops, or more conveniently  $\dot{V}_{ent}$ , the volume entrainment rate of fluid inside the vortex. If  $n_0$  is the ambient drop number density, the evolution of the number of drops,  $N$ , in the vortex is given by:

$$\frac{dN}{dt} = n_0 \dot{V}_{ent} - N/\tau_{ev}. \quad (7)$$



This equation is valid only if the drops have enough time to enter the vortex without evaporating totally, that is,

$$\tau_{ev} > \frac{2\pi R_0 d_0}{\dot{V}_{ent}}.$$

For the purpose of evaluating  $N$ , a characteristic value for  $\tau_{ev}$  is chosen,  $\tau_{ev} = d_0^2/K_{ev}$ , where  $d_0$  is the initial drop diameter and  $K_{ev}$  is the  $D^2$ -law constant.  $\dot{V}_{ent}$  is assumed to be proportional to the outer radius of the vortex, and to the radial velocity of that structure. Classical results for turbulent mixing layers show that both outer vortex radius and the radial velocity are proportional to the mean longitudinal velocity of the vortex,  $u_0$  (see for example Dimotakis [19]). Thus one may write

$$\dot{V}_{ent} = \alpha_{ent} u_0^2. \quad (8)$$

Now,

$$\frac{dN}{dt} = \alpha_{ent} n_0 u_0^2 - \frac{K_{ev} N}{d_0^2}. \quad (9)$$

Considering that at  $t = 0$ ,  $R_0 = 0$ , the solution is

$$N = n_0 \alpha_{ent} u_0^2 \tau_{ev} \left[ 1 - \exp\left(-\frac{t}{\tau_{ev}}\right) \right].$$

This shows that  $N$  is an increasing function of time. This effect has thus to be considered in any model of combustion in a jet spray.

Another point of interest is the influence of small scale turbulence on the combustion of the cluster. The distance between the flame and the cluster ranges from 1% to 10% of the cluster radius. For the reference case, this ratio is about 5% and has to be compared with the ratios of turbulent scales calculated in the section describing the model and numerical method. It turns out that the flame-cluster distance is larger than the Kolmogorov scale and of the order of the Taylor microscale (in this case). One can thus conclude that small-scale turbulence will alter simultaneously the reaction zone and the closest drops. Even though the main reaction zone (the diffusion

flame) is small with respect to a characteristic small scale of turbulence, the complete structure including the closest drops, the cold fuel vapor and the diffusion flame cannot be considered thin with respect to the same characteristic scale.

However, the small scales may not be able to modify the dynamics of the drops. In our case, the Stokes number, based upon the flow time of the vortex is of order one. That is,

$$\text{St}(L_T) = \frac{\rho_l d_0^2 u'}{18\mu L_T} \approx 1.$$

One may calculate the ratio

$$\frac{\text{St}(L_T)}{\text{St}(\eta_k)} = \frac{u' \eta_k}{L_T u_k} = \frac{u' (\nu^3 \epsilon^{-1})^{1/4}}{L_T (\epsilon \nu)^{1/4}} = \text{Re}_T^{-1/2}$$

Thus,

$$\text{St}(\eta_k) = \text{Re}_T^{1/2} \text{St}(L_T) \gg 1.$$

This shows that the Kolmogorov eddies will have no effect on the trajectory of the drops, and more generally, the effect of the eddies will decrease with the size of these eddies.

## CONCLUSIONS

In this paper we have assumed that combustion is of the "group combustion" type, but we have allowed "individual (or internal) ignition" to occur, even though the resulting internal combustion was only approximately modeled. It turns out that in most cases, and especially for dense clusters, which were the focus of this study, this assumption was verified. However, internal combustion may not be neglected, especially during initiation. In fact, in our model where we identify the conditions at the cluster boundary with those at the edge of the sphere of influence, combustion always starts internally, at least for a very short time. In a more refined model describing the temperature profile inside the cluster, ignition would occur around the drops which are surrounded by the hottest gas. As the cluster cools, internal combustion cannot be sustained and an unsteady phase follows. Generally, the air initially inside the cluster is not totally depleted at the onset

of unsteady combustion. A diffusion flame then appears near the edge of the cluster. The diffusion flame turns out to be quasi-steady.

When the drops disappear, a fraction ranging from 1% to 30% of the initial mass of fuel has been burned. The critical parameters that determine the nature of the combustion (internal or external) are the drop number density, the cluster radius and the initial spinning rate of the drops. These last two parameters are related to the dynamics of the cluster and the transfer between the cluster and its surroundings, and were not studied in earlier investigations on combustion of groups of drops (see, for example, Zhuang et al. [20]). It was found that even a dense cluster is likely to burn internally if it is submitted to a strong centrifugal force. Since in the present model there is no difference made between the inner drops and the outer ones, the previous conclusion means that, in a strong vortex, at least the drops near the periphery may burn individually, even though they are densely packed.

The accumulation of a cold mixture of fuel and air between the flame and the cluster is also an interesting feature, and shows the complexity of the flame structure. It also explains why the flux of air to the flame seems more critical than the fuel flux.

The model could be improved by relaxing some assumptions. First, it would be desirable to calculate the temperature and mass fractions profiles inside the cluster as a function of the radial coordinate originating at the cluster center, since most changes occur in a very small region near the cluster boundary. Second, calculations could benefit from more realistic initial conditions, since some cases retained an unsteady aspect during the entire calculation time. The initial formation of the drop clusters in the vortices, and the following evolution of the vortices in the shear layer also require more modeling. Such a model will enable one to know, for example, the configuration of the drops in the large coherent structure, and the evolution of the number of drops in it. As was previously noticed, the various time scales involved are not well known yet. Well-characterized experimental observations will be required for model verification. In a recent experiment with a reacting spray, Goix

et al. [21] used fluorescence imaging and did not find any evidence of individual drop burning; they found instead thin, structured flame sheets surrounding groups of drops. This gives credibility to one of our assumptions, but further verifications of the present assumptions should be made in the future.

*The research described in this paper was carried out by the Jet Propulsion Laboratory, California Institute of Technology, under a contract with the National Aeronautics and Space Administration. One of the authors (Florian Fichot) was sponsored by the Société Européenne de Propulsion, and the research of the other two authors was funded by the U.S. Army Research Office, with Dr. David M. Mann acting as technical monitor through an interagency agreement with the National Aeronautics and Space Administration.*

#### \*REFERENCES

1. Lazaro, B. J., and Lasheras, J. C., *Twenty-second Symposium International on Combustion*, The Combustion Institute, Pittsburgh, 1989, pp. 1991-1998.
2. Crowe, C. T., Chung, J. N., and Troutt, T. R., *Prog. Combust. Sci.* 14:171-194 (1988).
3. Longmire, E. K., and Eaton, J. K., *J. Fluid Mech.* 236:217-257 (1992).
4. Bellan, J., and Harstad, K., *Twenty-third Symposium on Combustion*, The Combustion Institute, Pittsburgh, 1990, pp. 1375-1381.
5. Linan A., *Combust. Sci. Technol.* 14:95-117 (1976).
6. Rangel, R. H., and Continillo, G., *Twenty-fourth Symposium International on Combustion*, The Combustion Institute, Pittsburgh, 1992, pp. 1493-1501.
7. Karagozian, A. R., and Marble, F. E., *Combust. Sci. Technol.* 45:65-84 (1986).
8. Ghoniem, A. F., Knio, O. M., and Krishnan, A., *Twenty-third Symposium International on Combustion*, The Combustion Institute, Pittsburgh, 1990, pp. 699-705.
9. Allen, M. G., and Hanson, R. K., *Twenty-first Symposium (International) on Combustion*, The Combustion Institute, Pittsburgh, 1986, pp. 1755-1762.
10. Allen, M. G., and Hanson, R. K., *Opt. Eng.*, 25:12 1309-1311 (1986).
11. Mizutani, Y., Nakabe, K., Fuchihata, M., Akamatsu, F., Zaizen, M., and El-Emam, S. H., *Atomizat. Sprays* 3:125-135 (1993).
12. McDonnel, V. G., Adachi, M., and Samuelsen, G. S., *Combust. Sci. Technol.* 82:225-248 (1992).
13. McDonnel, V. G., Adachi, M., and Samuelsen, G. S., *Atomizat. Sprays* (in press).



14. Rudoff, R. C., Brena de le Rosa, A., Sankar, S. V., and Bachalo, W. D., 27th Aerospace Sciences Meeting, paper AIAA-89-0052.
15. Mao, C-P., Oechsle, V., and Chigier, N. A., presented at the Central and Western States Section Technical Meeting/The Combustion Institute, San Antonio, Texas, 1985.
16. Westbrook, C. K., and Dryer, F. L., *Cumbust. Sci. Technol.* 27:31-43 (1981).
17. Bellan, J., and Harstad, K., *Combust. Sci. Technol.* 53: 75-87 (1987).
18. Koshland, C. P., Ph.D. thesis, Stanford University, 1985.
19. Dimotakis, P. E., *ALAA J.* 24:11, 1791-1796 (1986).
20. Zhuang, C., Yang, B., Zhou, J., and Yang, H., *Twenty-first Symposium (International) on Combustion*, The Combustion Institute, Pittsburgh, 1988, pp. 647-653.
21. Goix, P. S., Cessou, A., and Stepowski, D., Spring Meeting of the Western States Section, 1992.

\*PLEASE OBTAIN REFERENCES FROM THE SOURCES LISTED.

Received 15 March 1993; revised 1 March 1994

## APPENDIX: ASSUMPTIONS AND CLUSTER MODEL

Since it would be cumbersome to present a detailed description of the assumptions used in this model in the main text, these assumptions are discussed here. Most of these assumptions have already been presented elsewhere [4].

The cluster of drops is monodisperse and the drop number density is assumed uniform. The concept of the spheres of influence is used to geometrically partition the cluster into interacting elements. The interstitial space is the space in the volume of the cluster between the spheres of influence. The outer boundary of the cluster is the envelope of the outer spheres of influence, whereas the inner boundary of the cluster is the envelope of the inner spheres of influence.

### Thermodynamic Cluster and Vortex Model

All spheres of influence in the cluster are assumed to behave in an identical way, independently of their position within the cluster. The gas in each sphere of influence is assumed quasi-steady with respect to the liquid phase because of the very small ratio between the gas and liquid densities. Unlike in the classical,

simplified theory of drop evaporation and combustion,  $\rho D$  is not assumed constant. The dependent variables in the gas phase satisfy the continuity equation and diffusion equations, and the temperature in the liquid phase is the solution of a transient conduction equation which takes into account the change in the heating time scale due to recirculation within the drop. The two sets of equations are coupled at the drop surface through boundary conditions stating the conservation of fluxes, as well as through the Langmuir-Knudsen kinetic evaporation law.

The solutions of the conservation equations for the gas also satisfy boundary conditions at the edge of the sphere of influence. The edge of the sphere of influence is the radial location at which a sphere touches the adjacent spheres. These values of the dependent variables at the edge of the sphere of influence are the solutions of the global conservation equations for the gas inside the cluster. The assumption is made that the dependent variables are uniform in the interstitial spaces, and that because of functional continuity their values are the same as those at the edge of the spheres of influence.

The gas outside the cluster is treated in a transient way because as evaporation proceeds the average density within the cluster approaches the gas density. Coupling with the gas in the inner vortex core (see below) and at the outer cluster boundary is performed through boundary conditions stating the conservation of all fluxes.

The gas is assumed ideal.

### Dynamic Model for Cluster and Vortex

The cluster of drops is embedded into a vortex, and the drops are being centrifuged by the vortex. Thus, very quickly after the initialization of motion, a ring (or shell) composed of drops and gas forms around the center of the vortex; this shell is the cluster of drops. The inner and outer surfaces of the cluster are calculated from the dynamics of the drops [4]. Separate equations are solved for the inner vortex core devoid of drops and these are coupled to the equations of the cluster at the



## EVAPORATION AND COMBUSTION OF A DROP CLUSTER

cluster (moving) inner boundary. Similar considerations are used to calculate the (moving) outer cluster boundary.

The drops and gas in the cluster move with different velocities which are the solutions of the fully coupled momentum equations for drops and gas. The drops and gas velocities have both a radial and a tangential component and the dynamic interaction between drops and gas occurs through the intermediary of a

drag force. The drag force, which was modeled elsewhere [4], is a function of the drop number density, the evaporation rate and the slip velocity. The drag coefficient used in the calculations was found by taking into account the "blowing" from the drops during evaporation.

The solutions of the four algebraic momentum equations are found by assuming that each component is the sum of an irrotational contribution and a solid body rotation.